
This is an electronic reprint of the original article.
This reprint may differ from the original in pagination and typographic detail.

Author(s): Kocourek, T. & Inkinen, S. & Pacherova, O. & Chernova, E. & Potucek, Z. & Yao, L. D. & Jelinek, M. & Dejneka, A. & van Dijken, S. & Tyunina, M.

Title: Effects of doping and epitaxy on optical behavior of NaNbO₃ films

Year: 2015

Version: Final published version

Please cite the original version:

Kocourek, T. & Inkinen, S. & Pacherova, O. & Chernova, E. & Potucek, Z. & Yao, L. D. & Jelinek, M. & Dejneka, A. & van Dijken, S. & Tyunina, M. 2015. Effects of doping and epitaxy on optical behavior of NaNbO₃ films. Applied Physics Letters. Volume 107, Issue 17. 172906/1-4. 0003-6951 (printed). DOI: 10.1063/1.4934850.

Rights: © 2015 AIP Publishing. This article may be downloaded for personal use only. Any other use requires prior permission of the authors and the American Institute of Physics. The following article appeared in Applied Physics Letters. Volume 107, Issue 17 and may be found at <http://scitation.aip.org/content/aip/journal/apl/107/17/10.1063/1.4934850>.

All material supplied via Aaltodoc is protected by copyright and other intellectual property rights, and duplication or sale of all or part of any of the repository collections is not permitted, except that material may be duplicated by you for your research use or educational purposes in electronic or print form. You must obtain permission for any other use. Electronic or print copies may not be offered, whether for sale or otherwise to anyone who is not an authorised user.



Effects of doping and epitaxy on optical behavior of NaNbO₃ films

T. Kocourek, S. Inkinen, O. Pacherova, E. Chernova, Z. Potucek, L. D. Yao, M. Jelinek, A. Dejneka, S. van Dijken, and M. Tyunina

Citation: [Applied Physics Letters](#) **107**, 172906 (2015); doi: 10.1063/1.4934850

View online: <http://dx.doi.org/10.1063/1.4934850>

View Table of Contents: <http://scitation.aip.org/content/aip/journal/apl/107/17?ver=pdfcov>

Published by the [AIP Publishing](#)

Articles you may be interested in

[Strain-controlled optical absorption in epitaxial ferroelectric BaTiO₃ films](#)

Appl. Phys. Lett. **106**, 192903 (2015); 10.1063/1.4921083

[Dual-enhancement of ferro-/piezoelectric and photoluminescent performance in Pr³⁺ doped \(K_{0.5}Na_{0.5}\)NbO₃ lead-free ceramics](#)

Appl. Phys. Lett. **105**, 042902 (2014); 10.1063/1.4891959

[Ferroelectric domain structure of anisotropically strained NaNbO₃ epitaxial thin films](#)

J. Appl. Phys. **115**, 204105 (2014); 10.1063/1.4876906

[Remanent-polarization-induced enhancement of photoluminescence in Pr³⁺-doped lead-free ferroelectric \(Bi_{0.5}Na_{0.5}\)TiO₃ ceramic](#)

Appl. Phys. Lett. **102**, 042907 (2013); 10.1063/1.4790290

[Effect of manganese doping on remnant polarization and leakage current in \(K 0.44 , Na 0.52 , Li 0.04 \) \(Nb 0.84 , Ta 0.10 , Sb 0.06 \) O 3 epitaxial thin films on Sr Ti O 3](#)

Appl. Phys. Lett. **92**, 212903 (2008); 10.1063/1.2937000

The logo for AIP APL Photonics is displayed in a white font on a red background. The letters 'AIP' are large and bold, followed by a vertical bar and the words 'APL Photonics' in a smaller font.

AIP | APL Photonics

APL Photonics is pleased to announce
Benjamin Eggleton as its Editor-in-Chief



Effects of doping and epitaxy on optical behavior of NaNbO_3 films

T. Kocourek,¹ S. Inkinen,² O. Pacherova,¹ E. Chernova,^{1,3} Z. Potucek,⁴ L. D. Yao,² M. Jelinek,¹ A. Dejneka,¹ S. van Dijken,² and M. Tyunina^{1,5,a)}

¹*Institute of Physics, Academy of Sciences of the Czech Republic, Na Slovance 2, Prague 8 CZ-18221, Czech Republic*

²*NanoSpin, Department of Applied Physics, Aalto University School of Science, P.O. Box 15100, FI-00076 Aalto, Finland*

³*Czech Technical University, Technická 2, Prague 6 CZ-166 27, Czech Republic*

⁴*Faculty of Nuclear Sciences and Physical Engineering, Czech Technical University, Trojanova 13, Prague 2 CZ-120 00, Czech Republic*

⁵*Microelectronics and Materials Physics Laboratories, University of Oulu, P.O. Box 4500, FI-90014 Oulun yliopisto, Finland*

(Received 11 September 2015; accepted 18 October 2015; published online 28 October 2015)

Cube-on-cube epitaxy of perovskite sub-cell of Pr-doped and undoped NaNbO_3 is obtained in 130-nm-thick films on top of $(\text{La}_{0.18}\text{Sr}_{0.82})(\text{Al}_{0.59}\text{Ta}_{0.41})\text{O}_3$ (001) substrates. Experimental studies show that the edge of optical absorption red-shifts and some interband transitions change in the films compared to crystals. Bright red luminescence is achieved at room-temperature under ultraviolet excitation in the Pr-doped film. An interband mechanism of luminescence excitation is detected in the film, which is in contrast to the intervalence charge transfer mechanism in the crystal. The results are discussed in terms of epitaxially induced changes of crystal symmetry and ferroelectric polarization in the films. It is suggested that the band structure and interband transitions in NaNbO_3 and the transition probabilities in the Pr ions can be significantly modified by these changes.

© 2015 AIP Publishing LLC. [<http://dx.doi.org/10.1063/1.4934850>]

Perovskite-structure oxide ferroelectric crystals possess high transparency and large index of refraction in the visible optical range, excellent nonlinear optical behavior, and high dielectric susceptibility. These optical properties enable numerous photonic and optoelectronic applications of ferroelectrics. Moreover, doping of ferroelectrics with lanthanide ions leads to room-temperature luminescence in the visible range. The luminescence can be stimulated optically, electrically, or mechanically, making doped ferroelectrics attractive for applications in light-emitting diodes, displays, and complex sensing-actuating systems. Advanced miniature integrated applications require high-quality and small-sized ferroelectrics, which can be achieved by the use of single-crystal-type epitaxial thin films instead of bulk crystals or ceramics. However, due to the film-substrate mismatch, heteroepitaxial films can acquire the structural phases and functional properties that differ significantly from those in bulk crystals.^{1–5} Thus, knowledge on how epitaxy influences the optical behavior of ferroelectrics is vital for many applications.

In this letter, we report on the combined effects of Pr-doping and epitaxy on room-temperature optical constants and luminescence in NaNbO_3 (NNO) films. NNO is an end member of advanced lead-free ferroelectric solid solutions $(\text{K},\text{Na})(\text{Nb},\text{Ta})\text{O}_3$ with the excellent piezoelectric properties and a unique diffractionless light propagation.^{6–8} Moreover, the red-color photoluminescence (PL) can be excited by ultraviolet radiation in the Pr-doped NNO crystals and $(\text{K},\text{Na})\text{NbO}_3$ ceramics.^{9–11} Bulk NNO possesses an orthorhombic crystal structure and exhibits an antiferroelectric

behavior at room temperature.^{12,13} When epitaxial NNO films are grown on top of cubic substrates, a monoclinic-type ferroelectric *r*-phase is expected to form in the films.² Here, such epitaxial Pr-doped and undoped NNO films are prepared. Bright red PL is achieved at room temperature in the Pr-doped films with a thickness of 130 nm. We show that, when compared to bulk crystals, the interband optical transitions and PL excitation spectra change in epitaxial films. We ascribe the observed behavior to a change of lattice symmetry and the presence of ferroelectric polarization in the epitaxial NNO films.

Pr-doped and undoped NNO films with a thickness of approximately 130 nm were grown onto $(\text{La}_{0.18}\text{Sr}_{0.82})(\text{Al}_{0.59}\text{Ta}_{0.41})\text{O}_3$ (LSAT) (001) single-crystal substrates (MTI Corp.), using the pulsed laser ablation from ceramic Pr-doped NNO and undoped NNO targets. The nominal content of Pr in the doped target was 1 mol. %. The deposition was performed at an elevated temperature of 973 K and an oxygen pressure of 20 Pa, while the pressure was adjusted to 800 Pa during the post-deposition cooling. The room-temperature crystal structure of the NNO films was studied by x-ray diffraction (XRD) and by high-resolution transmission electron microscopy (HRTEM). The XRD measurements were performed on a Bruker D8 diffractometer using the $\text{Cu K}\alpha$ radiation (Figure 1). HRTEM imaging and selected area electron diffraction (SAED) analysis were carried out on a JEOL 2200FS TEM with Cs correction, operated at 200 kV (Figure 2).

The structural analyses evidence a cube-on-cube-type epitaxy of the NNO perovskite cell with the NNO(00 l) planes parallel to the LSAT(00 l) planes, and the [100]NNO directions along the [100]LSAT directions. The lattice parameters of the films are estimated from the positions of

^{a)}Author to whom correspondence should be addressed. Electronic mail: marinat@ee.oulu.fi

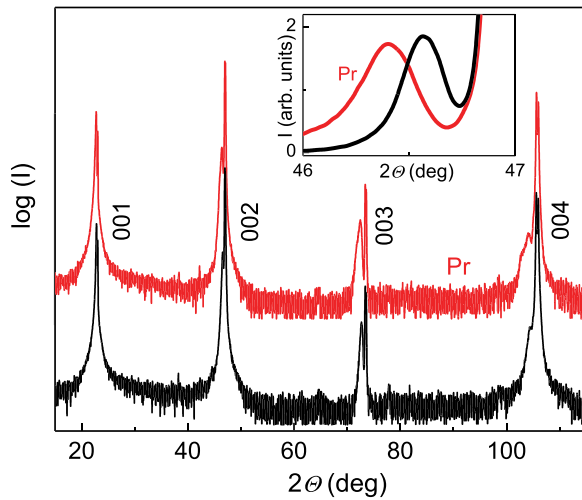


FIG. 1. Θ - 2Θ x-ray diffraction patterns in the undoped and Pr-doped (denoted by Pr in the plots) NNO films on LSAT(001) substrates. The positions of the (00 l) diffractions are marked. High-intensity narrow peaks are substrate diffractions. Inset shows NNO(002) diffractions.

Bragg diffractions using EVA software and taking the substrate as a reference. The out-of-plane lattice parameter c (normal to substrate surface) is ~ 3.901 Å in the undoped NNO film and ~ 3.914 Å in the Pr-doped NNO film. The theoretical NNO-LSAT lattice misfit is approximately 1% at the temperature of film growth. The observed columnar microstructure suggests a pronounced relaxation of the substrate-induced biaxial in-plane compressive strain in NNO during the high-temperature growth (Figure 2(a)). Since the coefficient of thermal expansion in pseudo-cubic perovskite sub-cell of NNO is considerably larger than that of LSAT, a tensile in-plane strain can additionally build up in the NNO film during the post-deposition cooling. The room-temperature lattice parameter c in the NNO film is smaller than the averaged parameter of the NNO bulk sub-cell, $a_{bulk} = (V_{bulk})^{1/3} \approx 3.905$ Å, where V_{bulk} is the sub-cell volume.¹⁴ Such an out-of-plane compression in the NNO film agrees with the discussed thermal strain. Compared with the undoped NNO film, the Pr-doped film has larger unit-cell volume. Since the Na^+ and Pr^{3+} ions have very similar ionic radii, it is accepted that Pr^{3+} substitutes Na^+ in NNO.⁹ An excess charge created at Na-site upon Pr-doping can lead to the increased unit-cell volume in the Pr-doped film. The revealed cube-on-cube-type epitaxy of NNO on LSAT suggests that the NNO films exhibit the theoretically predicted

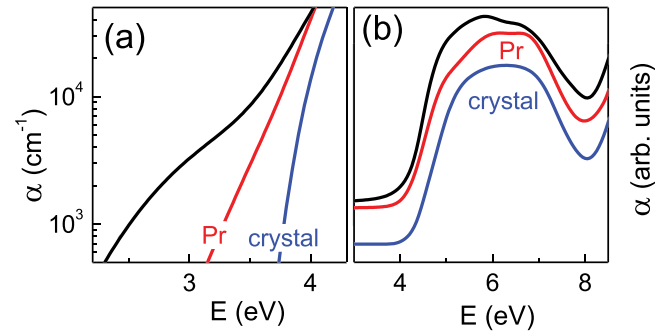


FIG. 3. The absorption coefficient α as a function of photon energy E in the undoped and Pr-doped (marked by Pr) epitaxial NNO films, and undoped reference NNO crystal. The logarithmic scale in (a) and the relative one in (b) are used for convenience of comparison.

r -state, where the ferroelectric polarization has non-zero components along all three crystal directions of the perovskite NNO sub-cell. Although the corresponding lattice distortions are difficult to detect here, the ferroelectric behavior has been experimentally confirmed in similar films.^{15–18} In particular, ferroelectric transition has been evidenced in epitaxial NNO films on LSAT.¹⁸

The optical constants in the NNO films were explored by variable-angle spectroscopic ellipsometry (VASE) using a VUV J. A. Woollam ellipsometer. The bare LSAT substrates and bulk undoped polydomain NNO crystal were studied as a reference. The ellipsometric angles Δ and ψ were measured at room temperature in vacuum (10^{-8} Pa) over a spectral range from 0.74 to 9.0 eV with a step of 0.02 eV and at angles of incidence 65° , 70° , and 75° . The data analysis was performed using the WVASE32 software package as described earlier.^{18–20} The spectra of the absorption coefficient α were extracted from the VASE data (Figure 3). As seen from Figure 3(a), the edge of absorption is shifted to lower energies in the films compared to the crystal. In order to quantify this red shift, the photon energy E_α for which the absorption coefficient equals $\alpha = 10^4 \text{ cm}^{-1}$ is estimated with an accuracy of ± 0.01 eV. The energy E_α is approximately 3.56, 3.75, and 3.96 eV in the undoped NNO film, Pr-doped NNO film, and undoped NNO crystal, respectively. Both the films and crystal exhibit broad absorption bands with the maxima $\alpha \approx 10^6 \text{ cm}^{-1}$ in the spectral range between 4 and 8 eV. However, the shapes of the spectra in this range are clearly different for the epitaxial films and crystal (Figure 3(b)), suggesting differences between inter-band optical transitions therein.

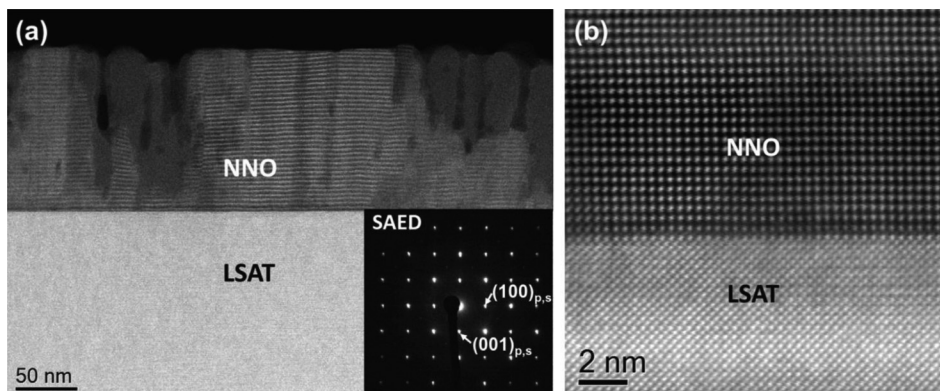


FIG. 2. (a) Cross-sectional TEM image and SAED pattern (inset) of the NNO/LSAT sample along the $[010]_{p,s}$ zone axis. The subscripts p and s denote the pseudocubic notation of NNO and cubic notation of LSAT, respectively. (b) HRTEM image from a specific column including interface.

The energies of the interband transitions were determined by analyzing the second derivatives of the dielectric function ($\epsilon = \epsilon_1 + i\epsilon_2$) and assuming two-dimensional critical points.^{21,22} The derivative spectra were obtained by numerical differentiation of the smoothed dielectric functions using Origin software.²³ The derivatives $d^2\epsilon_1/dE^2$ and $d^2\epsilon_2/dE^2$ (Figure 4) reveal a main spectral feature around 4.5 eV in the films and crystal. This feature comprises two lines: a stronger one at $\sim(4.4\text{--}4.5)$ eV and a weaker one at $\sim(4.7\text{--}4.9)$ eV. An obvious change in the films compared to the crystal is that the line at ~ 4.9 eV is shifted to lower energies and that its amplitude is suppressed. Moreover, additional features at ~ 6 eV are seen in the films.

The observed changes of the absorption edge and interband transitions in the epitaxial NNO films compared to the NNO crystal imply that the electronic band structure of NNO can be significantly affected by epitaxial growth and, less, by Pr-doping. The epitaxially induced monoclinic-type crystal structure, lattice strain, and ferroelectric polarization—all these factors can influence the band structure in the NNO films. A more detailed discussion can be found in Ref. 20. Next, we show that the epitaxy-related changes of crystal structure and ferroelectric polarization also impact the luminescence behavior of NNO.

The room-temperature PL emission spectra were measured using a grating monochromator (SPM 2, Carl Zeiss) and a cooled RCA 31034 photomultiplier (GaAs photocathode) operating in the photon-counting mode. The emission spectra were corrected for the spectral dependence of the apparatus response. A high-pressure Xe lamp and a double-grating Jobin Yvon DH 10UV monochromator were used for the excitation of PL. The Pr-doped NNO film is found to exhibit the bright red-colored PL, which can be readily seen by the naked eye. This red PL is excited by the ultraviolet radiation. We notice that in order to achieve such a bright luminescence in doped ferroelectric films, the required film thickness is usually 3–10 times larger.^{24–26}

The obtained spectrum of PL emission contains a strong narrow line at approximately 2 eV (wavelength 610 nm) in the Pr-doped film (Figure 5(a)), closely resembling that at 620 nm in the Pr-doped NNO crystal.⁹ Thus, also similar to the crystal, the red PL in the film can be ascribed to radiative

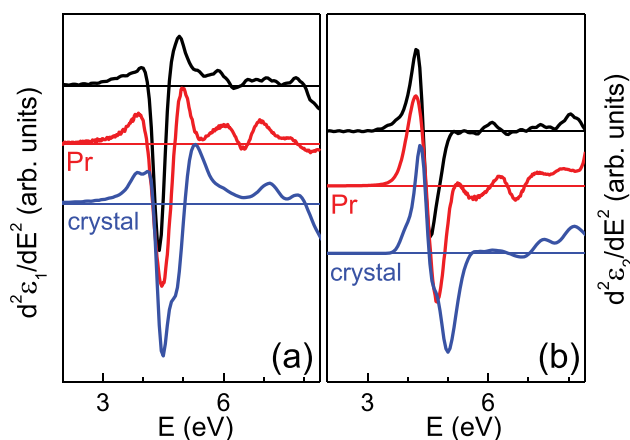


FIG. 4. The second derivatives of the dielectric functions, $d^2\epsilon_1/dE^2$ and $d^2\epsilon_2/dE^2$, as a function of photon energy E in the undoped and Pr-doped (marked by Pr) epitaxial NNO films, and undoped reference NNO crystal.

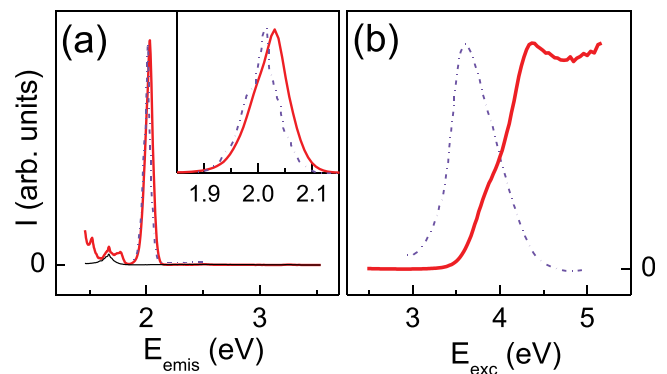


FIG. 5. (a) The emission spectra of luminescence excited at 4.37 eV (284 nm) in the Pr-doped (thick line) and undoped (thin line) NNO films. Inset shows the details of spectra around 2 eV. (b) The excitation spectrum of luminescence monitored at 2.03 eV (610 nm) in the Pr-doped NNO film. Dashed lines show the spectra in the Pr-doped NNO crystal (data taken from Ref. 9).

transitions between the 1D_2 excited state and the 3H_4 ground state of Pr^{3+} ions.⁹ The PL excitation is generally explained by the presence of an intervalence charge transfer state (IVCT) inside the bandgap. The existence of this state is indicated by a broad excitation spectrum centered at ~ 3.6 eV (344 nm) in the Pr-doped NNO crystal.⁹ The excitation spectrum of the red PL in the Pr-doped NNO film differs significantly from that in the crystal (Figure 5(b)). A closer inspection reveals a main excitation band centered at ~ 4.4 eV and a weaker one at ~ 3.8 eV in the film. The main band at ~ 4.4 eV can be directly related to the dominating interband transition evidenced by the analysis of derivatives (Figure 4). Although a transition at ~ 3.8 eV is difficult to clearly resolve in the derivative spectra, its interband nature, not connected to Pr-doping, is indicated by the large absorption coefficient at ~ 3.8 eV observed in the undoped and doped NNO films. The results suggest that the interband transitions in the NNO host are responsible for the excitation of the red PL in the Pr-doped NNO film. Interestingly, a trend from the IVCT excitation towards the band-to-band-dominated one has been found for PL in Pr-doped (Ca,Sr)TiO₃ ceramics, where it has been ascribed to an increase of the valence-band energy upon increasing Sr content.²⁷ As theoretically shown in Ref. 28, change of crystal symmetry and lattice strain can raise the valence-band energy in epitaxial ferroelectric films when compared to prototype crystals. Such an epitaxy-induced increase of the valence-band energy may be responsible for the band-to-band excitation in the Pr-doped NNO film in contrast to the IVCT in the crystal. Also it is worth mentioning that the presence of ferroelectric polarization can lead to an enhanced PL intensity in the epitaxial film. The lattice distortions connected to the ferroelectric polarization can lower crystal symmetry around the Pr^{3+} ions, and consequently, result in the increased probabilities for radiative transitions in these ions.²⁶ We anticipate that the PL intensity can be further enhanced in the Pr-doped NNO films by selecting appropriate substrates, which can enable epitaxial growth of thin films with a larger ferroelectric polarization.¹⁶

In conclusion, the optical constants and photoluminescence are experimentally studied in 130-nm-thick epitaxial

NNO and Pr-doped NNO films. Cube-on-cube epitaxy of the perovskite NNO cell on top of LSAT (001) is evidenced by XRD and HRTEM. The films exhibit a red-shift of the absorption edge and a change of some interband transitions compared to reference polydomain NNO crystal. The bright red photoluminescence is observed under ultraviolet excitation in the Pr-doped NNO film. The PL emission in the film resembles that in the crystal and is ascribed to the $^1D_2 \rightarrow ^3H_4$ transition of Pr^{3+} . The PL excitation in the film is found to be band-to-band-type, in contrast to the intervalence charge transfer mechanism in the crystal. The results imply that the band structure and interband transitions in NNO, and transition probabilities in Pr^{3+} can be significantly modified by epitaxially induced changes of crystal symmetry and ferroelectric polarization. Correspondingly, the epitaxial growth may be used to tune optical properties of thin films for photonic and optoelectronic applications.

The authors acknowledge support from the Grant Agency of Czech Republic (Grant No. 15–15123S), the Academy of Finland (Grant No. 260361), the Finnish Funding Agency for Innovation (Grant No. 400.31.2013), and the European Research Council (ERC-2012-StG 307502-E-CONTROL). HRTEM analysis was conducted at the Aalto University Nanomicroscopy Center (Aalto-NMC).

¹N. A. Pertsev, A. G. Zembilgotov, and A. K. Tagantsev, *Phys. Rev. Lett.* **80**, 1988 (1998).

²O. Diéguez, K. M. Rabe, and D. Vanderbilt, *Phys. Rev. B* **72**, 144101 (2005).

³C. Ederer and N. A. Spaldin, *Phys. Rev. Lett.* **95**, 257601 (2005).

⁴N. A. Pertsev and B. Dkhil, *Appl. Phys. Lett.* **93**, 122903 (2008).

⁵M. Tyunina, J. Narkilahti, M. Plekh, R. Oja, R. M. Nieminen, A. Dejneka, and V. Trepakov, *Phys. Rev. Lett.* **104**, 227601 (2010).

⁶Y. Saito, H. Takao, T. Tani, T. Nonoyama, K. Takatori, T. Homma, T. Nagaya, and M. Nakamura, *Nature* **432**, 84 (2004).

⁷E. DelRe, E. Spinazzi, A. J. Agranat, and C. Conti, *Nat. Photonics* **5**, 39 (2011).

⁸A. Sukhorukov, *Nat. Photonics* **5**, 4 (2011).

⁹P. Boutinaud, L. Sarakha, and R. Mahiou, *J. Phys.: Condens. Matter* **21**, 025901 (2009).

¹⁰H. Sun, D. Peng, X. Wang, M. Tang, Q. Zhang, and X. Yao, *J. Appl. Phys.* **111**, 046102 (2012).

¹¹Y. Wei, Z. Wu, Y. Jia, J. Wu, Y. Shen, and H. Luo, *Appl. Phys. Lett.* **105**, 042902 (2014).

¹²I. Lefkowitz, K. Lukaszewicz, and H. D. Megaw, *Acta Crystallogr.* **20**, 670 (1966).

¹³K. E. Johnston, J. M. Griffin, R. I. Walton, D. M. Dawson, P. Lightfoot, and S. E. Ashbrook, *Phys. Chem. Chem. Phys.* **13**, 7565 (2011).

¹⁴Yu. I. Yuzyuk, P. Simon, E. Gagarina, L. Hennem, D. Thiaudiere, V. I. Torgashev, S. I. Raevskaya, I. P. Raevskii, L. A. Reznitchenko, and J. L. Sauvajol, *J. Phys.: Condens. Matter* **17**, 4977 (2005).

¹⁵S. Yamazoe, H. Sakurai, M. Fukada, H. Adachi, and T. Wada, *Appl. Phys. Lett.* **95**, 062906 (2009).

¹⁶M. Tyunina and J. Levoska, *Appl. Phys. Lett.* **95**, 102903 (2009).

¹⁷Y. I. Yuzyuk, R. A. Shakhovoy, S. I. Raevskaya, I. P. Raevskii, M. ElMarssi, M. G. Karkut, and P. Simon, *Appl. Phys. Lett.* **96**, 222904 (2010).

¹⁸M. Tyunina, D. Chvostova, O. Pachterova, T. Kocourek, M. Jelinek, L. Jastrabik, and A. Dejneka, *Sci. Technol. Adv. Mater.* **15**, 045001 (2014).

¹⁹M. Tyunina, L. D. Yao, D. Chvostova, T. Kocourek, M. Jelinek, A. Dejneka, and S. van Dijken, *New J. Phys.* **17**, 043048 (2015).

²⁰M. Tyunina, D. Chvostova, L. D. Yao, A. Dejneka, T. Kocourek, M. Jelinek, and S. van Dijken, *Phys. Rev. B* **92**, 104101 (2015).

²¹P. Lautenschlager, M. Garriga, S. Logothetidis, and M. Cardona, *Phys. Rev. B* **35**, 9174 (1987).

²²P. Lautenschlager, M. Garriga, L. Vina, and M. Cardona, *Phys. Rev. B* **36**, 4821 (1987).

²³For details of data processing see <http://www.originlab.com/doc/Tutorials>.

²⁴H. Takashima, K. Ueda, and M. Itoh, *Appl. Phys. Lett.* **89**, 261915 (2006).

²⁵H. Takashima, K. Shimada, N. Miura, T. Katsumata, Y. Inaguma, K. Ueda, and M. Itoh, *Adv. Mater.* **21**, 3699 (2009).

²⁶J. Hao, Y. Zhang, and X. Wei, *Angew. Chem., Int. Ed.* **50**, 6876 (2011).

²⁷Y. Katayama, J. Ueda, and S. Tanabe, *J. Lumin.* **148**, 290 (2014).

²⁸R. F. Berger, C. J. Fennie, and J. B. Neaton, *Phys. Rev. Lett.* **107**, 146804 (2011).